J. Fluid Mech. (2004), *vol.* 505, *pp.* 309–321.
DOI: 10.1017/S0022112004008663 Printed in the United Kingdom

Characteristic lengths at moving contact lines for a perfectly wetting fluid: the influence of speed on the dynamic contact angle

By JENS EGGERS[1]† AND HOWARD A. STONE[2]

[1]Universität Gesamthochschule Essen, Fachbereich Physik, 45117 Essen, Germany
[2]Division of Engineering and Applied Sciences, Harvard University, Cambridge, MA 02138, USA

(Received 24 October 2002 and in revised form 10 September 2003)

It is common to relate the dynamic contact angle θ_d to the relative speed between the substrate and the contact line; theory suggests $\theta_d^3 \propto U$. In fact, available physical models show that the dynamic angle involves speed logarithmically and in a model-dependent manner. Experimental data consistent with this interpretation are cited.

1. Introduction

One area of fluid mechanics that has been the subject of a large admixture of analysis, experiment and speculation is the subject of the moving contact line. A typical situation, common in many coating processes, refers to the contact line at the intersection of solid, liquid and gas regions, where the three-phase line moves relative to a solid substrate. A basic question in this subject stems from the violation of the no-slip condition in the immediate neighbourhood of the three-phase line of contact (e.g. Huh & Scriven 1971; for reviews see Dussan V. 1979; de Gennes 1985; Kistler 1993). As a result, within the usual continuum analysis, the stress diverges as the contact line is approached and the energy per unit length of the moving contact line is unbounded. This result may be viewed as an embarrassment of continuum modelling, but, in fact, it does indicate the need for a small cutoff length scale in macroscopic theories, as well as some more input from the physics at smaller length scales to interpret properly the meaning of any such cutoff scale.

Perhaps the most basic feature of this problem is the aim to relate the local dynamic contact angle $\theta_d(x)$, which is the arc tangent of the slope of the interface at a distance x from the contact line, to the local speed U with which the contact line moves over the substrate. For the case of a perfectly wetting fluid (vanishing equilibrium contact angle $\theta_{eq} = 0$) and small θ_d, we find $\theta_d^3 \propto U$, which is known as Tanner's law. Theoretical justification for this result has been given (e.g. de Gennes 1985) and various generalizations have been offered. In dimensionless form, the speed is reported in terms of the capillary number $\mathscr{C} = U\eta/\gamma$, which measures the relative importance of viscous to surface tension forces, where η is the fluid viscosity and γ the interfacial tension. In fact, the functional form for the contact angle-speed relation is commonly written for small angles as $\theta_d^3(x) \approx 9\mathscr{C} \ln(x/\ell_{micro})$, where ℓ_{micro} is generally taken as a molecular length (e.g. Leger & Joanny 1992). Typically, the capillary number varies

† Present address: School of Mathematics, University of Bristol, University Walk, Bristol BS8 1TW, UK.

over many orders of magnitude; values $10^{-7} < \mathscr{C} < 10^{-1}$ are common. The prefactor multiplying the speed in this formula can be important for interpreting experimental data, and so it is reasonable to interrogate more closely the functional dependence on speed.

In this paper, we wish to comment on one aspect of the moving contact line problem that has been largely neglected and/or unappreciated. In particular, we note that detailed models for the perfectly wetting situation actually yield a dynamic contact angle versus speed relation

$$\theta_d^3(x) \approx 9\mathscr{C} \ln\left(\frac{x}{\ell_{micro}}\mathscr{C}^{\beta}\right), \tag{1.1}$$

where $\beta > 0$ depends on the physical model introduced in the neighbourhood of the contact line. We do not believe that it is necessarily appropriate simply to suppress the additional dependence on speed (i.e. $\mathscr{C}$) by replacing the argument of the logarithm by either $\ell_{macro}/\ell_{micro}$, where these two length scales are taken as constants, or x/ℓ_{micro}. Because of the large variation in $\mathscr{C}$, not including this additional factor of capillary number when using (1.1) to interpret dynamical experiments may lead to significant discrepancies between theory and experiment. Here, we outline the basic idea behind (1.1) and present experimental evidence that supports the above interpretation of a model-dependent value of β.

Another point that has received insufficient attention is the range of validity of equation (1.1). Near the contact line, (1.1) breaks down where x is of the same order as $\ell_{micro}\mathscr{C}^{-\beta}$. This restriction is evident as the general structure comes from a balance of viscous and surface tension forces alone. Not surprisingly, we estimate below that the microscopic scale is between several ångstroms and tens of ångstroms, depending on the microscopic forces assumed to be acting near the contact line.

Toward large scales, x is commonly taken to be a static scale such as the capillary length or the size of a spreading drop (de Gennes 1985). Nevertheless, it should be noted that the flow near a moving contact line often resembles a coating flow, similar to the classical problem studied by Landau and Levich (e.g. Levich 1962). This leads to the appearance of another, *dynamical* length scale, that can become much smaller than the capillary length as the capillary number is small, which is typically the case. Thus, a meaningful comparison between (1.1) and a macroscopic measurement of the dynamical contact angle might require a spatial resolution significantly below $1/10$ or even $1/100$ of the capillary length.

In the next section, we will introduce two different models commonly used to treat moving-contact-line problems such as a spreading drop or a tape plunging into a pool of fluid. Then, in § 3, we show that the lubrication equations corresponding to both models have similarity solutions for the interfacial shape that fix the functional dependence on the capillary number. Section 4 discusses the dynamical problem that equation (1.1) has to be matched to on an appropriate outer length scale. In § 5, we explain measurable consequences of the two models for the dynamic contact angle, and discuss an experiment that helps to distinguish between them. We close with a summary and possible directions of future work.

2. The model

The usual dynamic balance for the steady flow 'far' from the contact line involves capillary and viscous stresses. As the contact line is approached, the capillary-viscous flow leads to a stress singularity. A number of different physical effects have been

Mechanism	Reference
Van der Waals	Hervet & de Gennes (1984)
Navier slip	Huh & Scriven (1971)
Nonlinear slip	Thompson & Troian (1997)
Shear thinning	Gorodtsov (1990)
Diffuse interface	Seppecher (1996)
Generalized Navier slip	Shikmurzaev (1997)

TABLE 1. Different models for the flow in the neighbourhood of the contact line, with representative references.

suggested to relieve the singularity, and these either account for the fact that on very small length scales van der Waals forces act to maintain a finite-thickness liquid layer on the solid substrate, or that at very high shear rates the boundary conditions and the transport coefficients of the fluid are likely to be altered. Which model is appropriate might depend on the physical system at hand, or be a combination of the above. In table 1, we provide a short overview of proposed physical models for flow in the neighbourhood of a contact line; see also McKinley & Ovryn (1998). There has been a considerable effort to base the understanding of the contact-line physics on a microscopic particle-based description (see for example Koplik, Banavar & Willemsen 1989; Ruijter, Blake & de Coninck 1999; Abraham, Cuerno & Moro 2002). The so-called 'diffuse interface' model (see e.g. Seppecher 1996; Chen, Ramé & Garoff 2000; Pomeau 2002) represents an intermediate approach in that it attempts to model the inner structure of the liquid–gas interface, but uses a continuum model.

Below, we restrict our attention to two different models which have proved particularly popular. The results are sufficient to highlight the measurable differences between different physical mechanisms. In model I, due to de Gennes and coworkers (e.g. Hervet & de Gennes 1984; de Gennes 1985), van der Waals forces are taken into account, so, very close to the contact line, there is a balance between surface tension and van der Waals stresses alone. In model II, proposed for example by Huh & Mason (1977) and Hocking (1977), the fluid is allowed to slip across the solid surface over a small slip length.

For simplicity, we consider only the case of perfectly wetting fluids, i.e. of zero equilibrium contact angle. Consistent with the local balances, the interface near the contact line remains nearly flat and we can use lubrication theory to describe the fluid motion. This approach amounts to a significant simplification of the mathematical treatment relative to the full two-dimensional flow problem (Cox 1986), but agrees with the full calculation when the dynamic contact angle is small. There are numerous indications that the small-angle theory in fact remains valid for slopes of order unity. For example, $\theta_d^3/9$ in equation (1.1) differs by only 2% from the full expression (Cox 1986), derived without the benefit of lubrication theory, up to a slope of 1. Also, Fermigier & Jenffer (1991) reported that small-angle theory holds experimentally up to an angle of 100°, in agreement with earlier experiments by Hoffman (1975).

To be able to describe an experiment like a flat plate plunging with velocity U into a reservoir of fluid (see figure 1), it is necessary to include other terms beyond the lubrication terms close to the contact line; namely, we keep the full curvature term and include gravity. By doing this, the model is able to describe the crossover to a purely static, horizontal surface far away from the dynamical region. A basic unit of length is the capillary length $\ell_c = \sqrt{\gamma/g\rho}$, which dictates the scale of the interface

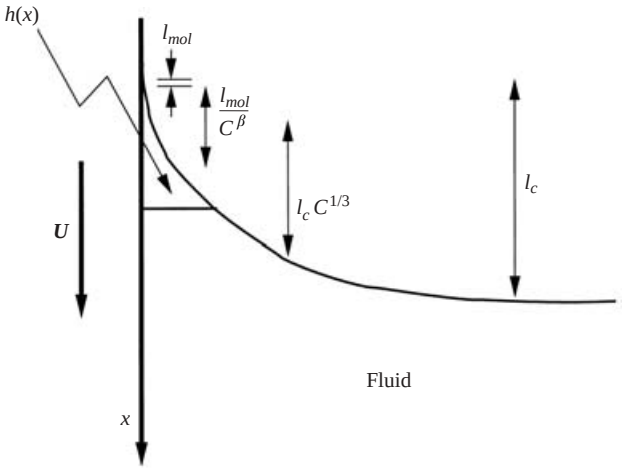

FIGURE 1. A typical application involving a moving contact line: a plate plunges with velocity U into a liquid-filled container; the capillary length $\ell_c = \sqrt{\gamma/\rho g}$. Since we assume wetting fluids, the meniscus creeps up the plate opposite to the direction of motion and a non-zero dynamic contact angle $\theta_d(x)$ is established. In the experiment of Marsh, Garoff & Dussan V. (1993) referred to below, the plate is replaced by a cylinder which can be tilted at different angles α. We also schematically indicate the different length scales relevant for this problem.

curvature far away from the contact line. In the van der Waals model I, which accounts for pressure variations owing to capillary, van der Waals and gravitational forces, the equation for the stationary profile $h(x)$ (cf. figure 1) is

$$\frac{3\mathscr{C}}{h^2} = \kappa' + 3a^2\frac{h'}{h^4} - \ell_c^{-2}, \tag{2.1}$$

where $\kappa(x)$ is the curvature and a prime refers to differentiation with respect to x. Note that a positive $\mathscr{C}$ corresponds to the plate plunging into the fluid. A brief derivation of model I, as well as model II below, is given in Appendix A. The microscopic length parameter a, defined by

$$a^2 = \frac{A}{6\pi\gamma}, \tag{2.2}$$

measures the strength of van der Waals forces relative to interfacial forces and is typically very small (of the order of ångstroms).

Another distinct approach for the flow near the contact line is to introduce slip at the boundary, consistent with allowing the contact line to move parallel to the wall at a finite speed; the slip is a function of the shear rate. The simplest such law, introduced by Navier in the same paper that also enunciated the Navier–Stokes equation (Navier 1823), is

$$u|_{y=0} - U = \lambda\frac{\partial u}{\partial y}\bigg|_{y=0} \tag{2.3}$$

(see also Huh & Scriven 1971). Here, U is the speed of the moving boundary, $y=0$ denotes the solid–liquid boundary, and λ is the so-called slip length. A more complicated version of (2.3), in which λ is itself a nonlinear function of the shear rate, has been proposed in Thompson & Troian (1997). A standard calculation (Appendix A),

leads to the analogue of (2.1) for the slip model II,

$$\frac{3\mathscr{C}}{h^2} = \kappa' - 3\lambda\frac{\left(\ell_c^{-2} - \kappa'\right)}{h} - \ell_c^{-2}. \tag{2.4}$$

The slip length λ is usually considered to be of the order of tens of ångstroms.

3. Scaling solutions near the contact line

We now focus on the immediate neighbourhood of the contact line, which we assume to be at $x = 0$. Owing to the flatness of the interface, we can assume that $\kappa \approx -h''$ and gravitational influences can be neglected, but dynamical (viscous) effects have to be included. In the case of model I, (2.1) reduces to

$$\frac{3\mathscr{C}}{h^2} = -h''' + 3a^2\frac{h'}{h^4}. \tag{3.1}$$

To make the dependence on parameters explicit, we note that (3.1) has the exact scaling solution

$$h(x) = \frac{a}{\mathscr{C}^{1/3}}\phi_1\left(a^{-1}\mathscr{C}^{2/3}x\right), \tag{3.2}$$

where ϕ_1 depends on the similarity variable $\xi_1 = a^{-1}\mathscr{C}^{2/3}x$ and satisfies the equation

$$\frac{3}{\phi_1^2} = -\phi_1''' + 3\frac{\phi_1'}{\phi_1^4}. \tag{3.3}$$

Similarly, the lubrication approximation for model II gives

$$\frac{3\mathscr{C}}{h^2} = -h''' - \frac{3\lambda}{h}h'''. \tag{3.4}$$

In this case, the scaling solutions are

$$h(x) = \lambda\phi_2\left(\lambda^{-1}\mathscr{C}^{1/3}x\right), \tag{3.5}$$

where the similarity variable is now $\xi_2 = \lambda^{-1}\mathscr{C}^{1/3}x$ and the similarity equation is

$$\frac{3}{\phi_2^2} = -\phi_2''' - \frac{3}{\phi_2}\phi_2'''. \tag{3.6}$$

Far away from the contact line in units of the microscopic lengths a and λ, respectively, the solutions should be the same, resulting from a balance of classical viscous forces and surface tension. Indeed, as $\xi \to \infty$, we find to leading order

$$\phi_{1,2}(\xi) \approx 3^{2/3}\xi\left[\ln(\xi b_{1,2})\right]^{1/3} \quad (\xi \gg 1), \tag{3.7}$$

where the numerical constants $b_{1,2}$ have to be determined by numerical integration starting from the contact line.

The boundary condition at the contact line incorporates the wetting behaviour of the fluid, and uses the fact that, on microscopic length scales, static forces will dominate over dynamical ones. In the presence of van der Waals forces (model I), and for a perfectly wetting fluid, a thin liquid film precedes the contact line (Voinov 1977; Hervet & de Gennes 1984), in which surface tension and van der Waals forces are balanced. The existence of such a 'precursor' film has been confirmed experimentally by several groups, and its properties compare favourably with theory (e.g. Kavehpour, Ovryn & McKinley 2003). Instead of integrating (3.1) or (3.3) from the location of the contact line, solutions of (3.3) have to be matched to the precursor film. Following

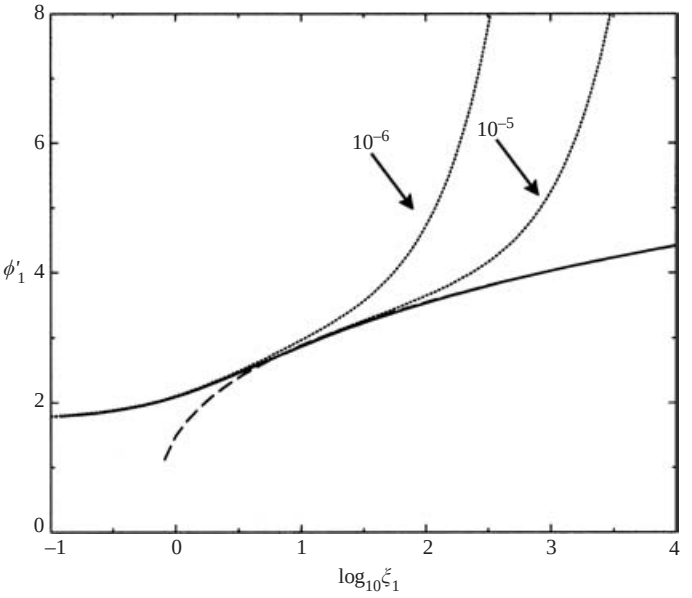

FIGURE 2. The rescaled slope $\phi_1' = h' a^{-1} \mathscr{C}^{1/3}$ versus $\log_{10}(\xi_1) = \log_{10}(a^{-1}\mathscr{C}^{2/3}x)$ for $\mathscr{C} = 10^{-5}, 10^{-6}$ in the geometry of figure 1. The ratio $a/\ell_c = 10^{-8}$. The full line is a solution of (3.1), the dashed line corresponds to the asymptotic form (3.7). The two dotted lines are solutions of the full system (2.1) including gravity, marked with their values of the capillary number. Note that for the smaller capillary number, the size of the overlap region where the asymptotic form (3.7) can be applied has shrunk to zero.

Hervet & de Gennes (1984), we are going to match $\phi_1(x)$ to a 'maximal' film solution, corresponding to very strong wetting, whose thickness only goes to zero at (minus) infinity. This maximal solution very closely approximates precursor film solutions of (3.3) having finite length (Hervet & de Gennes 1984). To leading order, the maximal film solution is of the form

$$\phi_1(\xi_1) = -\frac{1}{\xi_1} + \epsilon \exp\left\{\xi_1^3/\sqrt{3}\right\}; \tag{3.8}$$

further details are to be found in Appendix B. Using (3.8) as an initial condition with adjustable parameter ϵ, we integrate (3.3) toward $\xi_1 \to \infty$. The parameter ϵ is fixed to select the solution with vanishing curvature at infinity. Figure 2 compares this solution with the asymptotic form (3.7). We plot the rescaled slope ϕ_1' from the solution of (3.3) as the full curve and the corresponding prediction from (3.7) with $b_1 = 1.44$ as the dashed curve. After accounting for differences in normalization, this numerical value for b_1 differs significantly from $b_1 = 0.4 \times 3^{1/6} \approx 0.48$ given in de Gennes (1985). We believe the difference is simply due to the large values of ξ necessary for integration until a true asymptotic value is reached.

Model II, on the other hand, does not include a precursor film, but describes a macroscopic film that extends directly down to $\phi_2(0) = 0$. A vanishing equilibrium contact angle $\theta_{eq} = 0$ can thus be implemented by taking the boundary condition $\phi_2(0) = \phi_2'(0) = 0$ at the contact line and integrating (3.6) toward $\xi_2 \to \infty$. The corresponding value of b_2 for the case of the Navier slip law was given in Hocking

(1992). Thus the two constants, which establish the form of the interface profile, are

$$b_1 \cong 1.44, \quad b_2 \cong 3^{1/3}\exp(0.74/3) \cong 1.85. \tag{3.9}$$

4. Crossover to Landau–Levich-type behaviour

We now estimate the range of validity of the solution (3.7) as we move farther away from the contact line. These ideas have close analogy to the classical analysis of Landau and Levich of a dynamical lubrication film (Levich 1962). Evidently, the contact-line physics plays no role far away from the contact-line, so the relevant lubrication equation is

$$\frac{3\mathscr{C}}{h^2} = -h''', \tag{4.1}$$

which is to be matched to a static profile at large distances. This equation has the general solution

$$h(x) = \ell\mathscr{C}^{\alpha_1+1/3} f(x/(\ell\mathscr{C}^{\alpha_1})), \tag{4.2}$$

which has to be matched to a static meniscus on the capillary scale, with a curvature of the order of ℓ_c^{-1}. This implies $\alpha_1 = 1/3$ and $\ell = \ell_c$, so that we have

$$h(x) = \ell_c\mathscr{C}^{2/3} f\left(x\Big/\left(\ell_c\mathscr{C}^{1/3}\right)\right), \tag{4.3}$$

which suggests that the crossover will occur on a scale $\ell_c\mathscr{C}^{1/3}$, on which the logarithmic dependence in (3.7) for the slope begins to fail.

The crossover to scaling of the form of (4.3) is demonstrated in figure 2, by showing a full solution of (2.1), rescaled according to (3.2). Results are given for two (small) values of the capillary number differing by a factor of ten. Again, the free parameter in the maximal film solution (3.8) is used to shoot for the flat interface corresponding to the surface of the fluid-filled container. For small values of ξ_1, the solution corresponds to the lubrication form given before, while on a scale $x/\ell_c \approx \mathscr{C}^{1/3}$ the transition to the Landau–Levich region is observed. In rescaled coordinates ξ_1 the location of this crossover should thus be proportional to $\mathscr{C}$ itself, as is clearly seen from figure 2. We have chosen the smaller of the two values of $\mathscr{C}$ such that the region over which the asymptotic form (3.7) of the interface can be applied is zero, to highlight possible problems in comparing asymptotic solutions with experimental data. To interpret the measured dynamical contact angle, equation (3.7) is no longer sufficient, but the full solution of the similarity equation (3.3) has to be considered.

5. Comparison with experiment

It is common practice in the literature (e.g. de Gennes 1985; Cox 1986) to consider the derivative of the profile $h(x)$, evaluate it at some macroscopic distance from the contact line $x = \ell_{macro}$, and to interpret the slope of the interface in terms of the so-called 'dynamical contact angle', $\tan\theta_d(x) = \mathrm{d}h/\mathrm{d}x$. This approach is the common one taken in experiments. Thus, using the solution (3.7) in the similarity forms (3.2) and (3.5) for models I and II, respectively, and neglecting lower-order terms, we obtain

$$\theta_{dyn}^3(x) = 9\mathscr{C}\ln(\ell_{macro}/L_{1,2}), \tag{5.1}$$

where $L_{1,2}$ are microscopic lengths appropriate for each model. There are two fundamental issues with this approach. First, depending on the experimental system it is not clear what is the best choice for ℓ_{macro}. Namely, it needs to be significantly smaller than the scale on which the logarithmic law (5.1) breaks down. This scale, as

we just showed, may itself be given dynamically by $\ell_c \mathscr{C}^{1/3}$. Therefore, it is in general not sufficient to make ℓ_{macro} smaller than the linear size of a system such as the drop size.

Secondly, what is usually taken as a fixed microscopic length $L_{1,2}$ is actually strongly dependent on the capillary number. Namely, the two models give

$$L_1 = a\mathscr{C}^{-2/3}/b_1, \qquad L_2 = \lambda\mathscr{C}^{-1/3}/b_2, \tag{5.2}$$

as established in (3.2) and (3.5), respectively. Thus it is impossible to interpret $L_{1,2}$ directly in terms of some fixed microscopic length near the contact line, but rather it is a dynamical quantity. In particular, the $\mathscr{C}$-dependence that appears in the microscopic length is different in the two models. This appears to be significant, since comparing the $\mathscr{C}$-dependence potentially allows us to distinguish between different microscopic models from a macroscopic measurement.

A number of experiments with perfectly wetting fluids come to mind for such a comparison. Chen & Wada (1989) imaged the whole profile near the contact line of a spreading droplet and so provided the first experimental confirmation of the full functional form of (5.1). However, owing to the small range of capillary numbers studied, it is difficult to distinguish between the two lengths $L_{1,2}$ defined in (5.2). Below we will therefore concentrate on another experiment (Marsh *et al.* 1993), which allowed $\mathscr{C}$ to be varied over more than two orders of magnitude. These authors measured the dynamic contact angles on a cylinder plunging at an angle into a liquid bath, and essentially used the form (5.1) to fit the whole shape of the interface close to the contact line, but included static contributions to account for the effects of surface tension and gravity away from the contact line. (Note that instead of the third power on the left-hand side, they used a more complicated function $g(x)$, which becomes $g(x) \approx x^3/9$ for small arguments. This limit is relevant for the small-angle case we are studying here.) This approach leaves out dynamical effects of the kind predicted by Landau and Levich (Levich 1962), which are important on an intermediate scale between the microscopic ones and the capillary length, and should be taken into account in a more refined theory. Marsh *et al.* (1993) treat the microscopic interface angle at the contact line (called θ_{act} in their paper) as another free, and possibly $\mathscr{C}$-dependent, parameter, to be determined from experiment. From their fitting procedure, the authors conclude that $\theta_{act} = 0$, consistent with the model assumption $\theta_{act} = \theta_{eq} = 0$ we have made from the outset.

From the fit of (5.1) to their data, Marsh *et al.* (1993) extract a length L, which is found to depend significantly on capillary number, as suggested by (5.2). They also report L to be independent of the tilt angle α within experimental error, which further emphasizes that the response is dominated by local features. In figure 3, we present a plot of the measured length as a function of capillary number, and compare it with the slopes suggested by the van der Waals model I and the Navier slip model II, respectively. Although it is difficult to draw firm conclusions owing to the large scatter in the data, 2/3 seems to be favoured. Using the two different fits plotted in figure 3, we are also able to determine the cutoff lengths a and λ, assuming that the corresponding physical mechanism is really relevant for the particular materials involved. We find $a \approx 4\,\text{Å}$ for the van der Waals model and $\lambda \approx 30\,\text{Å}$ for the slip model. Using the value of $A = 10^{-20}\,\text{J}$ (Russel, Saville & Schowalter 1989) for the Hamaker constant for water and an adjacent solid surface, and $\gamma = 0.07\,\text{N m}^{-1}$, we find $a = \sqrt{A/(6\pi\gamma)} \approx 1\,\text{Å}$, consistent with the above value. However, it is important to keep in mind that there is no reason why a single cutoff mechanism should necessarily dominate in the experiment, which would lead to still other exponents. Additional

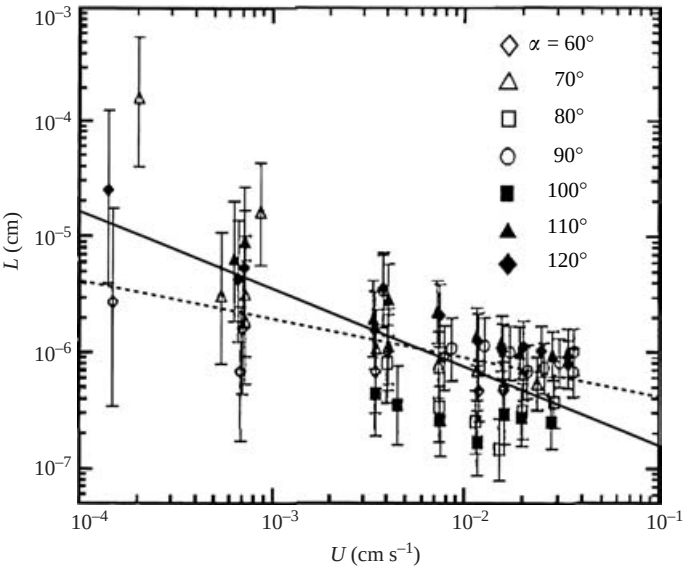

FIGURE 3. A plot of the microscopic length L, taken from figure 4 of Marsh *et al.* (1993), as a function of the speed U. Their L is the equivalent of $L_{1,2}$ as given in (5.1). The angle α refers to different tilts of the solid relative to the liquid surface. To make a comparison with the dynamical length sales $L_{1,2}$ as given in (5.2), we have added to the figure the solid and the dashed lines with slope 2/3 and 1/3, respectively.

mechanisms for relieving the contact-line singularity are given in table 1; which is the dominant mechanism could also depend on capillary number and, in particular, on the type of solid substrate or fluid involved.

6. Conclusions

We have considered flow local to a moving contact line using a lubrication approach. Our basic message has been to indicate that the appearance of logarithmic corrections in capillary number to the usual 'Tanner's law', $\theta_d^3 \propto \mathscr{C}$, are a general feature of the mechanical response. The interpretation of the results is that the 'microscopic' length scale that is involved when supplying a small-scale cutoff to relieve the well-known stress singularity in the moving contact-line problem is a dynamical (speed-dependent) quantity. Experimental data consistent with this interpretation are cited, and microscopic parameters that come from the comparison with different theories agree with physical considerations. In droplet-spreading problems where the contact angle is a function of time, the logarithmic dependence on capillary number shows up as an additional factor in the expression for the drop radius, that depends logarithmically on time (Hocking 1992; Giacomelli & Otto 2002).

It is interesting to note that the speed-dependent cutoff scale is a special property of the zero contact angle (perfectly wetting) case. For example, Hocking (1992) has investigated the slip model in the case of finite θ_{eq} in a manner analogous to § 3. He finds a cutoff length of

$$L_{sl} = 3\lambda/\theta_{eq}, \tag{6.1}$$

while de Gennes, Hua & Levinson (1990) find

$$L_{vdw} = a/\left(2\theta_{eq}^2\right), \tag{6.2}$$

in the case that van der Waals forces are important in the contact-line region. Thus, while there are still differences between the two models, they will be much harder to distinguish experimentally, since we would have to determine the absolute value of a constant inside the logarithm. Note that the divergence of both (6.1) and (6.2) in the limit $\theta_{eq} \to 0$ predicts the trouble of the perfectly wetting case.

Since important applications of contact-line theories apply to angles up to 180°, it would be useful to extend the lubrication theory considered here to a full two-dimensional treatment of the flow in the corner region, as done by Cox (1986). However, Cox explicitly excludes the case of small- or zero-equilibrium contact angles, thus avoiding the singularities mentioned in the preceding paragraph. It would therefore be worth including the possibility of a speed-dependent cutoff in the two-dimensional calculation. This means that the dynamical contact angle has the scaling form $\theta_d = f(\mathscr{C}, x/L_{1,2})$, where $L_{1,2}$ is one of the dynamical length scales defined by (5.2), with corresponding forms for the velocity field as well. Such a theory might be able to explain more recent experiments (Chen *et al.* 1995) on moving contact lines performed at higher capillary numbers, yielding dynamical contact angles of up to 155°.

Furthermore, the velocity of the contact line relative to the substrate is, in general, not perpendicular to the contact line, as highlighted in recent experiments of droplets running down an inclined plane (Podgorski, Flesselles & Limat 2001). In this case, the flow is truly three-dimensional, and it may no longer be sufficient to simply project the velocity onto the normal to the contact line (Blake & Ruschak 1979). Such a three-dimensional description would be necessary to complete our understanding of corner singularities that form at the back of running drops (Stone *et al.* 2002; Limat & Stone 2004), and may apply to a range of other contact-line phenomena as well.

We thank Cyprien Gay, Pirouz Kavehpour, Laurent Limat, Gareth McKinley, Thomas Podgorski and David Quéré for helpful conversations. H. A. S. thanks the Harvard MRSEC for partial support of this research.

Appendix A. Derivation of lubrication equations

Here, we briefly recall the derivation of the interface, or lubrication, equations for thin viscous films (Levich 1962). For pressure-driven flow along the surface and absorbing hydrostatic pressure variations into the pressure p, the velocity parallel to the plate can be represented as a second-order polynomial

$$u = a_0 + a_1 y + y^2 \frac{p'}{2\eta}, \tag{A 1}$$

where y is the distance normal to the plate. At the free surface $y = h(x)$, shear gradients $\partial u/\partial y$ vanish, giving $a_1 = -p'h/\eta$. Finally, from the slip condition (2.3) we have $a_0 = U - \lambda p'h/\eta$.

Since the contact line is stationary, the mass flux through the film is zero everywhere, $\int_0^h u(y)\,\mathrm{d}y = 0$, and thus

$$0 = (U - \lambda p'h/\eta)h - p'h^3/3\eta \tag{A 2}$$

is the equation for the film profile $h(x)$. In the presence of van der Waals forces, the dynamic pressure in the liquid is

$$p = \gamma\kappa - \frac{A}{6\pi h^3} - g\rho x, \tag{A 3}$$

where A is Hamaker's constant. Substituting (A 3) into (A 2) and assuming $\lambda = 0$ gives (2.1), while $A = 0$ at finite λ leads to (2.4).

Appendix B. Expansion for the maximal film

Here, we give some more details on the solution of (3.1) for the 'maximal film' of Hervet & de Gennes (1984). The general form of the film profile is

$$\phi_0 = \frac{1}{\xi} \sum_{i=0}^{\infty} \frac{a_i}{\xi^{6i}}, \tag{B 1}$$

where we denote the similarity variable by ξ. This expansion has no free parameters, as the values of the coefficients a_i are obtained directly from substituting (B 1) into (3.1). We find

$$a_0 = -1, \quad a_1 = -2/5, \quad a_2 = -1764/275, \ldots. \tag{B 2}$$

However, there is a one-parameter family of solutions of (3.1) that decay for $\xi \to -\infty$. This solution is found by linearizing around the base solution (B 1), i.e. $\phi(\xi) = \phi_0(\xi) + \delta(\xi)$:

$$\delta\left(6\phi_0 + 4\phi_0^3\phi_0'''\right) - 3\delta' + \delta'''\phi_0^4 = 0. \tag{B 3}$$

Equation (B 3) is solved using a WKB-type ansatz,

$$\delta(\xi) = \epsilon \exp\left\{\frac{\xi^3}{\sqrt{3}} + \ldots\right\}. \tag{B 4}$$

The $O(\xi^0)$ contribution in the exponent turns out to be a logarithm, so the full structure is

$$\delta = \frac{\epsilon}{\xi^2} \exp\left\{\sum_{i=0}^{\infty} \frac{b_i \xi^{3-3i}}{\sqrt{3}}\right\}, \tag{B 5}$$

and the coefficients are found to be

$$b_0 = 1, \quad b_2 = 0, \quad b_3 = 32/15, \quad b_4 = 9\sqrt{3}/5, \ldots. \tag{B 6}$$

Thus the general form of the solution in the film region is

$$\phi(\xi) = \phi_0(\xi) + \delta, \tag{B 7}$$

with a single free parameter ϵ. An alternative description would be an expansion of the form

$$\phi(\xi) = \sum_{i=1}^{\infty} \frac{c_i}{\xi^i}, \tag{B 8}$$

with $c_1 = -1$ and c_2 a free parameter. However, the convergence of the asymptotic series (B 8) turns out to be very poor, as perhaps is to be expected from the structure of the WKB solution.

REFERENCES

Abraham, D. B., Cuerno, R. & Moro, E. 2002 Microscopic model for thin film spreading. *Phys. Rev. Lett.* **88**, 206101(1)–(4).

Blake, T. D. & Ruschak, K. J. 1979 A maximum speed of wetting. *Nature* **282**, 489–491.

Chen, H.-Y., Jasnow, D. & Viñals, J. 2000 Interface and contact line motion in a two-phase fluid under shear flow. *Phys. Rev. Lett.* **85**, 1686–1689.

Chen, J.-D. & Wada, N. 1989 Wetting dynamics near the edge of a spreading drop. *Phys. Rev. Lett.* **62**, 3050–3053.

Chen, Q., Ramé, E. & Garoff, S. 1995 The breakdown of asymptotic hydrodynamic models of liquid spreading at increasing capillary number. *Phys. Fluids* **7**, 2631–2639.

Cox, R. G. 1986 The dynamics of the spreading of liquids on a solid surface. Part 1. Viscous flow. *J. Fluid Mech.* **168**, 169–194.

Dussan V., E. B. 1979 On the spreading of liquids on solid surfaces: static and dynamic contact lines. *Annu. Rev. Fluid Mech.* **11**, 371–400.

Fermigier, M. & Jenffer, P. 1991 An experimental investigation of the dynamic contact angle in liquid–liquid systems. *J. Colloid Interface Sci.* **146**, 226–241.

de Gennes, P. G. 1985 Wetting: statics and dynamics. *Rev. Mod. Phys.* **57**, 827–863.

de Gennes, P. G., Hua, X. & Levinson, P. 1990 Dynamics of wetting: local contact angles. *J. Fluid Mech.* **212**, 55–63.

Giacomelli, L. & Otto, F. 2002 Droplet spreading: intermediate scaling law by PDE methods *Commun. Pure Appl. Maths* **55**, 217–254.

Gorodtsov, V. A. 1990 Spreading of a film of nonlinearly viscous liquid over a horizontal smooth surface. *J. Engng Phys.* **57**, 879–884.

Hervet, H. & de Gennes, P. G. 1984 Dynamique du mouillage: films précurseurs sur solid 'sec'. *C.R. Acad. Sci. Paris* II **299**, 499–503.

Hocking, L. M. 1977 A moving fluid interface. Part 2. The removal of the force singularity by a slip flow. *J. Fluid Mech.* **79**, 209–229.

Hocking, L. M. 1992 Rival contact-angle models and the spreading of drops. *J. Fluid Mech.* **239**, 671–681.

Hoffman, R. L. 1975 A study of the advancing interface. *J. Colloid Interface Sci.* **50**, 228–241.

Huh, C. & Mason, S. G. 1977 The steady movement of a liquid meniscus in a capillary tube. *J. Fluid Mech.* **81**, 401–419.

Huh, C. & Scriven, L. E. 1971 Hydrodynamic model of steady movement of a solid/liquid/fluid contact line. *J. Colloid Interface Sci.* **35**, 85–101.

Kavehpour, H. P., Ovryn, B. & McKinley, G. H. 2003 Microscopic and macroscopic structure of the precursor layer in spreading viscous drops. *Phys. Rev. Lett.* **91**, 196104(1)–(4).

Kistler, S. 1993 Hydrodynamics of wetting. In *Wettability* (ed. J. C. Berg). Marcel Dekker, New York.

Koplik, J., Banavar, J. R. & Willemsen, J. F. 1989 Molecular dynamics of fluid flow at solid surfaces. *Phys. Fluids* A **1**, 781–794.

Leger, L. & Joanny, J. F. 1992 Liquid spreading. *Rep. Prog. Phys.* **55**, 431–486.

Levich, V. G. 1962 *Physicochemical Hydrodynamics*. Prentice–Hall.

Limat, L. & Stone, H. A. 2004 Three-dimensional lubrication model of a contact line corner singularity. *Europhys. Lett.* **65**, 365–371.

McKinley, G. H. & Ovryn, B. 1998 An interferometric investigation of contact line dynamics in spreading polymer melts and solutions. In *Proceedings of the Fourth Microgravity Fluid Physics and Transport Phenomena Conference*, Cleveland, Ohio.

Marsh, J. A., Garoff, S. & Dussan V., E. B. 1993 Dynamic contact angles and hydrodynamics near a moving contact line. *Phys. Rev. Lett.* **70**, 2778–2781.

Navier, C. L. 1823 (appeared in 1827) Sur les lois du mouvement des fluides. *Mem. Acad. R. Sci. France* **6**, 389–440.

Podgorski, T., Flesselles J. M. & Limat, L. 2001 Corners, cusps, and pearls in running drops. *Phys. Rev. Lett.* **87**, 036102(1)–(4).

Pomeau, Y. 2002 Recent progress in the moving contact line problem: a review. *C.R. Mec.* **330**, 207–222.

Ruijter, M. J., Blake, T. D. & De Coninck, J. 1999 Dynamic wetting studied by molecular modeling simulations of droplet spreading. *Langmuir* **15**, 7836–7847.

Russel, W. B., Saville, D. A. & Schowalter, W. R. 1989 *Colloidal Suspensions*, p. 148, table 5.3. Cambridge University Press.

Seppecher, P. 1996 Moving contact lines in the Cahn–Hilliard theory. *Intl J. Engng Sci.* **34**, 977–992.

Shikhmurzaev, Y. D. 1997 Moving contact lines in liquid/liquid/solid systems. *J. Fluid Mech.* **334**, 211–249.

Stone, H. A., Limat, L., Wilson S. K., Flesselles, J. M. & Podgorski, T. 2002 Corner singularity of a contact line moving on a solid substrate. *C. R. Phys.* **3**, 103–110.

Thompson, P. A. & Troian, S. M. 1997 A general boundary condition for liquid flow at solid surfaces. *Nature* **389**, 360–362.

Voinov, O. V. 1976 Hydrodynamics of wetting [English translation]. *Fluid Dyn.* **11**, 714–721.

Voinov, O. V. 1977 Inclination angles of the boundary in moving liquid layers [English translation]. *J. Appl. Mech. Tech. Phys.* **18**, 216–222.